USE OF THE ELECTROCHEMICAL MICROCELL TECHNIQUE FOR STUDYING PITTING CORROSION AT WELDED JOINTS OF LEAN DUPLEX STAINLESS STEEL UNS S32304*

Dalila Chaves Sicupira[1]
Ronaldo Cardoso Júnior[2]
Alexandre Queiroz Bracarense[3]
Gerald Frankel[4]
Vanessa de Freitas Cunha Lins[5]

Abstract
A pitting corrosion study of welded joints of lean duplex stainless steel (LDSS) UNS S32304 has been performed. LDSS S32304 thick plates were welded by different processes commonly employed in equipment and piping construction: SMAW (Shielded metal arc welding), GMAW (Gas metal arc welding) and FCAW (Flux cored arc welding). The electrochemical behavior of different weldment zones (fusion zone (FZ), base metal (BM) and heat affected zone (HAZ)) was characterized both independently using an electrochemical microcell and together through whole sample analysis. The electrochemical method applied was performed in acidified glycerin, a process fluid of the biodiesel industry. The results were correlated to the microstructural features of the materials. Based on the results, is possible to conclude that the breakdown potential (E_b) of the fusion zone (FZ) was higher than the E_b obtained for the heat affected zone (HAZ). In general, top samples show higher breakdown potential than root samples and also the samples welded using filler metal 2209 has a better anodic behavior than the filler metal 2307. According to the results, GMAW welding process with 2209 as filler metal was revealed as the optimum chosen for application of 2304 duplex stainless steels in this case.
Keywords: Pitting corrosion; LDSS; Welding process; Microcell.

[1] *Chemical, master, PhD student, Dept. of Chemical Engineering, Federal University of Minas Gerais, Belo Horizonte, MG, Brazil*
[2] *Product Manager at ESAB, Contagem, MG, Brazil*
[3] *Physicist, Dr., professor, Dept. of Mechanical Engineering, Federal University of Minas Gerais, Belo Horizonte, MG, Brazil*
[4] Materials Science and Engineering*, Dr., professor,* Dept. of Materials Science and Engineering, The Ohio State University, *Columbus, OH, USA.*
[5] Chemical Engineering*, Dr., professor, Dept. of Chemical Engineering, Federal University of Minas Gerais, Belo Horizonte, MG, Brazil.*

1 INTRODUCTION

The number of applications for duplex stainless steel increases steadily and new alloys are continuously developed. Lately, the main focus has been on lean duplex grades, and the fluctuating alloying element prices (especially Ni and Mo) during the last decade has accelerated the development and the amount of applications for these steels [1].
The study of the corrosion resistance of this material can minimize costs related to corrosion in different types of industry in which it may be used, for example, in the biodiesel industry. The history of the biodiesel industry reveals a significant number of faults (holes in pipes) caused by corrosion in acidic medium, that cause production losses and, consequently, economic losses. Although several studies related to the effect of heat input and thermal cycles on the microstructure of pipeline steels have been performed [1-3,8,9], there are few studies related to corrosion of LDSS in biodiesel plants.
The weldability of this type of duplex steel is generally good when using slightly over-alloyed filler metal as ISO 2307 N L or ISO 2209 N L [1]. However, the fusion welding process required for assembling the construction modifies the ferrite/austenite phase balance (1:1) in duplex stainless steels and promotes the intermediate phase's precipitation in the welded joints. The main consequence of this phenomenon is that corrosion resistance and mechanical properties of these materials are dramatically affected, particularly in the heat affected zone (HAZ) [10-12].
General and pitting corrosion of pipeline steels have been the subject of previous studies [2,3]. The most severe pitting is usually reported for the welded area with different rates of pit growth measured for the fusion zone, HAZ, and the base metal [4]. Corrosion resistance of the HAZ is reported to be highly dependent on the thermal cycle experienced by the base metal [5].
Microelectrochemical methods are powerful techniques to study localized corrosion processes on small areas of passive metals. Many works apply microelectrodes to study the working areas in the µm- nm range [7,13,14].
In this context, the objective of this work is to compare the corrosion resistance of LDSS UNS S32304 plates welded by processes commonly employed in equipment and piping construction as SMAW (Shielded metal arc welding), GMAW (Gas metal arc welding) and FCAW (Flux cored arc welding) in acidified glycerin, a co-product of biodiesel industry.

2 MATERIAL AND METHODS

2.1 Sample Preparation

This research is a continuation of the work done by Cardoso Junior [6], in which the samples were welded. Measurements were performed on welded joints of 2304 type stainless steel (Ni: 3.63 wt.%, Cr: 22.45, Mn: 1.35, S: 0.0004, Si: 0.39, P: 0.028, Mo: 0.44, N: 0.113 and C: 0.019).
The welded samples were cut transversely to the welding direction, to make possible the evaluation of the fusion zone (FZ), the heating affected zone (HAZ) and the base metal (BM) and for the both region of the sample, root (R) and top (T). From these cuts were taken specimens of approximately 5x30x5mm, as shown in Figure 1.

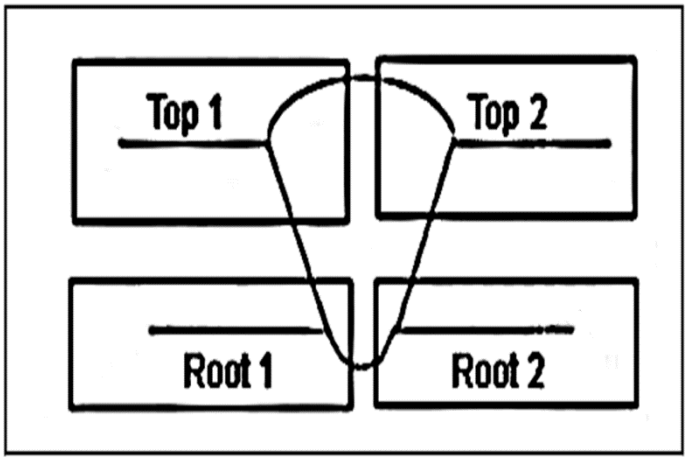

Figure 1. Representation of cutting samples for localized corrosion test.

The samples were mounted in epoxy resin and the electrical contact was made by welding a copper wire on the back of the sample. Also these samples were ground using 180, 320, 400 and 600 grit and stored in desiccators.

2.2 Microstructure Analysis

Before the electrochemical measurements, microstructural examination of specimens was conducted using a light optical microscope (Olympus PME 3, LECO). After polishing, the specimens were then electrolytically etched in 10% (m/v) oxalic acid electrolyte at 6 V for 60 s.

2.3 Electrochemical Technique

The local electrochemical behavior of specimens was studied at room temperature using the electrochemical microcell technique. This technique utilized a glass micro-capillary filled with the electrolyte, as shown in Figure 2.

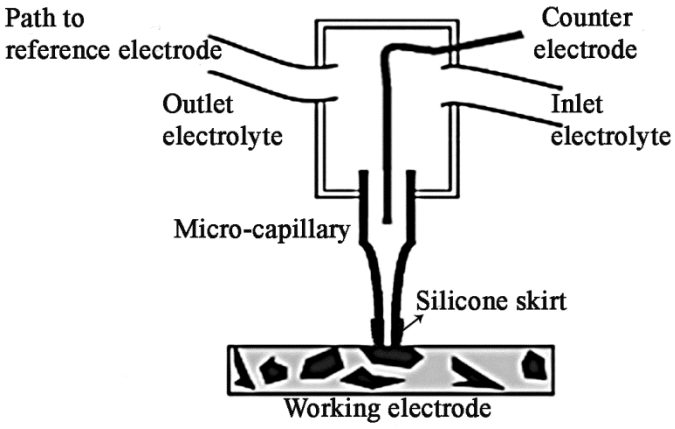

Figure 2. Schematic drawing of the microcell.

The microcapillary tip was sealed to the specimen surface with a layer of silicone rubber. The entire setup was placed in a faradic cage. The diameter of the microcapillary tip was 200micron, the counter electrode was a platinum wire and a saturated calomel electrode (SCE) was used as reference.

The tests were carried out in acidic glycerin (glycerin + methanol + water + hydrochloric acid) at pH= 5.8. Open circuit potential (OCP) was allowed to stabilize for a period of 5 minutes and the cyclic potentiodynamic polarization curves were then measured at a scan rate 5 $mV.s^{-1}$. Such precautions were taken to minimize test durations, in order to avoid any issues with cell leakage, or the establishment of concentration gradients in the capillary. It was discussed by Birbilis and Buchheit [7] that the nominal cell resistance (responsible for iR–drop) is comparatively high with respect to other systems, with values approaching 10kΩ recorded. However, since the absolute currents measured during testing rarely approched values up to 10^{-7} A, ohmic drop was considered negligible for potentiodynamic testing, since it would be nominally confined to under 1mV. The scanning direction was reversed when the current density reached 5 $mA.cm^{-2}$. Three replicate tests of each measurement were performed.

3 RESULTS AND DISCUSSION

The fusion zone structure (Figure 3a) consists of austenite grains in the form of Widmanstätten plates precipitates within a matrix of ferrite and showed higher proportions of austenite in the fusion zone than in HAZ, as expected. There is also apparent secondary phase precipitation in the ferrite matrix. Two morphologies of secondary austenite precipitates have been created (small white needle and island types), and some black patches of secondary phases (chromium nitrides) primarily within the ferrite grains. In general, it was observed similar microstructure for each welded sample analyzed.

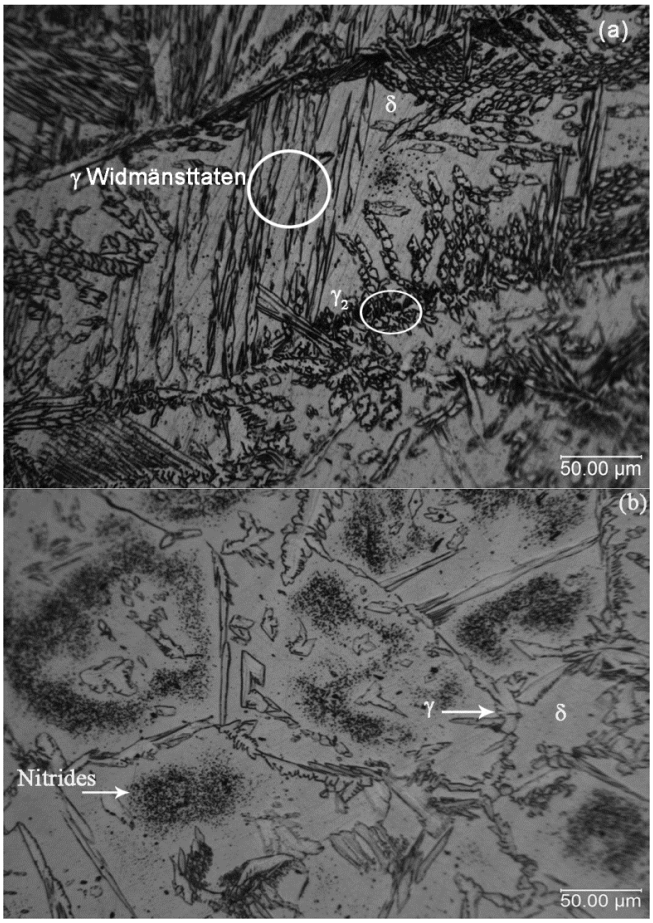

Figure 3. Optical microstructure of FZ (a) and HAZ (b) for SMAW top region (2307 as filler metal).

The open circuit potential and breakdown potential were evaluated by cyclic polarization test for each different region (BM, HAZ and FZ). Figures 4, 5 e 6 show the results obtained for samples welded by SMAW, GMAW and FCAW process respectively. The OCP values and breakdown potentials of as-received and samples welded by SMAW, GMAW and FCAW process are presented in Tables 1, 2 and 3 respectively.

Table 1. Experimental data for SMAW process

Sample	OCP (mV)	E_b (mV)	E_b Deviation (mV)
SMAW 2307 R FZ	-118	230	23
SMAW 2307 R HAZ	-135	84	10
SMAW 2307 T FZ	-118	471	116
SMAW 2307 T HAZ	-241	114	5
SMAW 2209 R FZ	-40	387	63
SMAW 2209 R HAZ	-118	137	23
SMAW 2209 T FZ	-82	587	8
SMAW 2209 T HAZ	-76	207	9
2304 as received	-137	142	63

Table 2. Experimental data for GMAW process

Sample	OCP (mV)	E_b (mV)	E_b Deviation (mV)
GMAW 2307 R FZ	-82	302	2
GMAW 2307 R HAZ	-88	226	16
GMAW 2307 T FZ	-76	231	25
GMAW 2307 T HAZ	-73	167	15
GMAW 2209 R FZ	-97	446	39
GMAW 2209 R HAZ	-143	272	22
GMAW 2209 T FZ	-64	354	59
GMAW 2209 T HAZ	-130	194	29
2304 as received	-137	142	63

Table 3. Experimental data for FCAW process

Sample	OCP (mV)	E_b (mV)	E_b Deviation (mV)
FCAW 2307 R FZ	-113	552	32
FCAW 2307 R HAZ	-144	179	3
FCAW 2307 T FZ	-109	302	11
FCAW 2307 T HAZ	-131	160	32
FCAW 2209 R FZ	-94	481	36
FCAW 2209 R HAZ	-164	260	16
FCAW 2209 T FZ	-22	490	25
FCAW 2209 T HAZ	-90	251	21
2304 as received	-137	142	63

It is apparent that, in general, the OCP values for the as received sample were more negative than the ones for welded samples (Table 1, 2, 3). However, comparing different regions for the welded samples, is possible to note that OCP values for the FZ region were more positive that the ones for HAZ region. This may interpreted as

better corrosion resistance of these samples, meaning that for the HAZ region the anodic reactions become dominant at higher potentials compared to those of FZ region.

The anodic polarization curves provide useful information concerning the potential range over which a material is susceptible to pitting corrosion. Figures 4, 5 and 6 show the cyclic potentiodynamic polarization curves of the welded UNS S32304 steel in acidified glycerin medium for the three analyzed zones, using microcell technique.

All curves presented a current plateau; the highest value was for the FZ. For the filler metal 2209 compared to the 2307, the pitting potential was shifted towards more noble potentials and presented the widest passive zone which is attributed to the highest Mo and Ni contents in its composition. This could be a sign of a good pitting corrosion resistance for these samples. The higher content of δ-ferrite in the HAZ could explain the less noble pitting potentials; δ-ferrite can be detrimental because of its susceptibility to attack in chloride medium [15]. Comparing, root and top samples, is possible to note that for SMAW and FCAW welding process, top samples show higher breakdown potential than root samples. This fact can be explained based on the smaller dilution of the filler metal for the top of the welded samples. However, in the case of samples welded by GMAW process, the root was more resistance than the top. This welding process does not have slag formation, that protect the fusion zone of nitrogen lose.

From the facts commented above it becomes confirmed that samples welded using filler metal 2209 has a better anodic behavior than the filler metal 2307; mostly due to the content and stabilizing role of Mo.

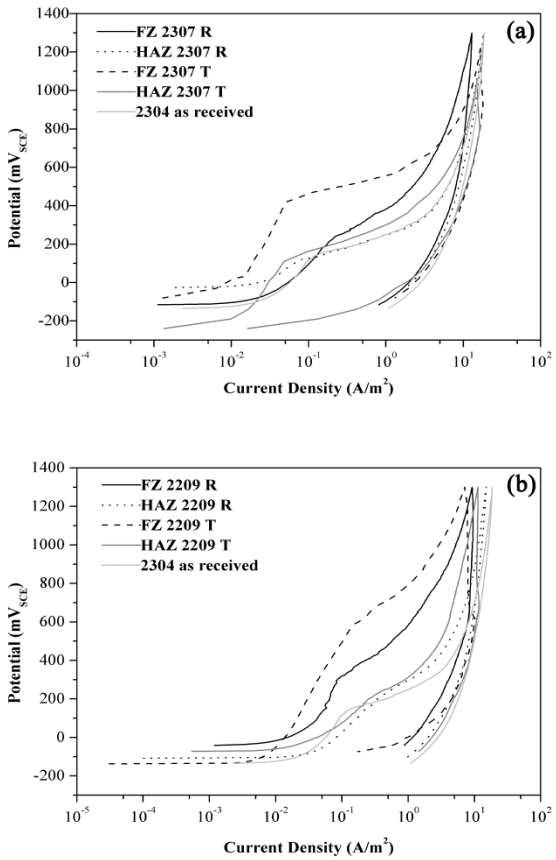

Figure 4. Cyclic Potentiodynamic polarization curves for SMAW process: (a) 2307 as filler metal and (b) 2209 as filler metal.

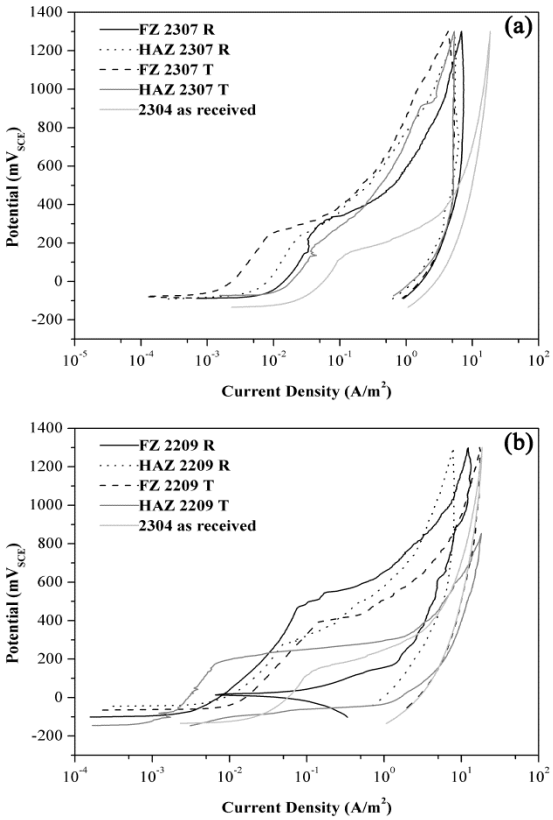

Figure 5. Cyclic Potentiodynamic polarization curves for GMAW process: (a) 2307 as filler metal and (b) 2209 as filler metal.

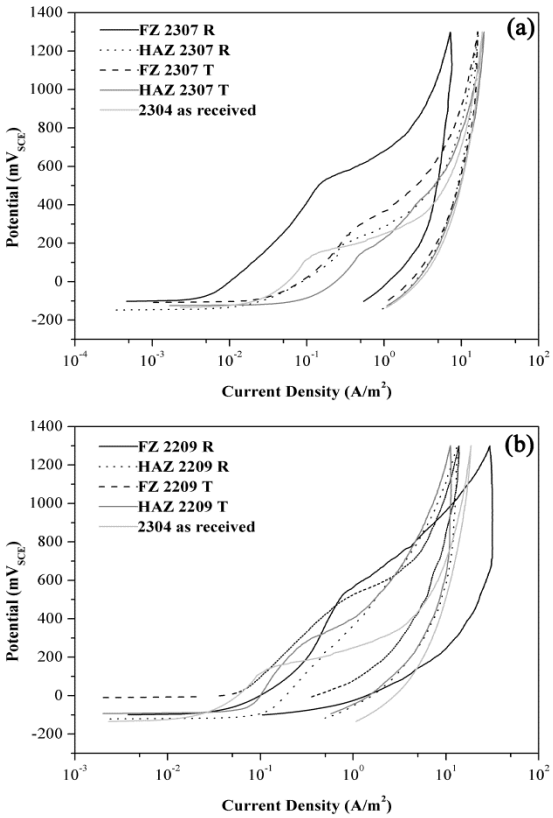

Figure 6. Cyclic Potentiodynamic polarization curves for FCAW process: (a) 2307 as filler metal and (b) 2209 as filler metal.

4 CONCLUSION

- The E_b of the fusion zone were higher than the E_b obtained for the heat affected zone.
- The E_b values of the HAZ for SMAW samples were lower than the values obtained for the HAZ of samples welded using GMAW and FCAW.
- Comparing, root and top samples, in the case SMAW and FCAW welding process, top samples showed higher breakdown potential than root samples. However, for GMAW samples, the root region was more resistance than the top.
- The samples welded using filler metal 2209 had a better anodic behavior than the filler metal 2307.
- GMAW welding process with 2209 as filler metal was revealed as the optimum chosen for application of 2304 duplex stainless steels in this case.

REFERENCES

1 Westin EM. Microstructure and properties of welds in the lean duplex stainless steel LDX 2101. Doctoral Thesis in Materials Science. Stockholm, Sweden: 2010.

2 Eliyan FF, Alfantazi A. Corrosion of the heat-affected zones (HAZs) of API-X100 pipeline steel in dilute bicarbonate solutions at 90°C – An electrochemical evaluation. Corrosion Science. 2013; 74: 297-307.

3 Mohammadi F, Eliyan FF, Alfantazi A. Corrosion of simulated weld HAZ of API X-80 pipeline steel. Corrosion Science. 2012; 63: 323-333.

4 Chaves IA, Melchers RE. Pitting corrosion in pipeline steel weld zones. Corrosion Science. 2011; 53: 4026-4032.

5 Yang Y, Yan B, Li J, Wang J. The effect of large heat input on the microstructure and corrosion behavior of simulated heat affected zone in 2205 duplex stainless steel. Corrosion Science. 2011; 53: 3756-3763.

6 Cardoso Junior R, Bracarense AQ, Campos FR, Souza CS, Silveira DM, Lins VFC. Avaliação da soldagem multipasse de chapas espessas de aços inoxidáveis lean duplex UNS S32304 soldadas pelos processos SMAW, GMAW e FCAW - Parte 1: Propriedades Mecânicas. Soldagem e Inspeção. 2012; 17: 306-316.

7 Birbilis N, Buchheit RG. Electrochemical characteristics of intermetallic phases in aluminum alloys. Journal of electrochemical society. 2005; 152: B140 – B151.

8 Chen L, Tan H, Wang Z, Li J, Jiang Y. Influence of cooling rate on microstructure evolution and pitting corrosion resistance in the simulated heat-affected zone of 2304 duplex stainless steels. Corrosion Science. 2012; 58: 168-174.

9 Tan H, Wang Z, Jiang Y, Yang Y, Deng B, Song H, Li J. Influence of welding thermal cycles on microstructure and pitting corrosion resistance of 2304 duplex stainless steels. Corrosion Science. 2012; 55: 368-377.

10 Garcia-Garcia DM, Garcia-Anton J, Igual-Murioz A, Blasco-Tamarit E. Effect of cavitation on the corrosion behavior of welded and non-welded duplex stainless steel in aqueous LiBr solutions. Corrosion science. 2006; 48: 2380-2405.

11 Ferro P, Tiziani A, Bonollo F. Influence of induction and furnace postweld heat treatment on corrosion properties of SAF 2205 (UNS 31803). Welding Journal. 2008; 87: 298-306.

12 Muthupandi V, Srinivasan PB. Effect of weld metal chemistry and heat input on the structure and properties of duplex stainless steel welds. Materials Science Engineering A.2003; 358: 9-16.

13 Vignal V, Krawiec H, Heintz O, Oltra R. The use of local electrochemical probes and surface analysis methods to study the electrochemical behaviour and pitting corrosion of stainless steels. Electrochimica Acta. 2007; 5: 4994-5001.

14 Krawiec H, Vignal V, Oltra R. Use of the electrochemical microcell technique and the SVET for monitoring pitting corrosion at MnS inclusions. Electrochemistry Communications. 2004; 6: 655-660.
15 Garcia C, Martin F, Tiedra P, Blanco Y, Lopez M. Pitting corrosion of welded joints of austenitic stainless steels studied by using an electrochemical minicell. Corrosion Science. 2008; 50: 1184-1194.